THE ROYAL SOCIETY

Published online 29 December 2004

The structure of the rigor complex and its implications for the power stroke

K. C. Holmes[1*], R. R. Schröder[1], H. L. Sweeney[2] and Anne Houdusse[3]

[1]*Max Planck Institute for Medical Research, 69120 Heidelberg, Germany*
[2]*Department of Physiology, University of Pennsylvania School of Medicine, 3700 Hamilton Walk, Philadelphia, PA 19104-6085, USA*
[3]*Structural Motility, Institut Curie CNRS, UMR144 26 rue d'Ulm, 75248 Paris cedex 05, France*

Decorated actin provides a model system for studying the strong interaction between actin and myosin. Cryo-energy-filter electron microscopy has recently yielded a 14 Å resolution map of rabbit skeletal actin decorated with chicken skeletal S1. The crystal structure of the cross-bridge from skeletal chicken myosin could not be fitted into the three-dimensional electron microscope map without some deformation. However, a newly published structure of the nucleotide-free myosin V cross-bridge, which is apparently already in the strong binding form, can be fitted into the three-dimensional reconstruction without distortion. This supports the notion that nucleotide-free myosin V is an excellent model for strongly bound myosin and allows us to describe the actin–myosin interface. In myosin V the switch 2 element is closed although the lever arm is down (post-power stroke). Therefore, it appears likely that switch 2 does not open very much during the power stroke. The myosin V structure also differs from the chicken skeletal myosin structure in the nucleotide-binding site and the degree of bending of the backbone β-sheet. These suggest a mechanism for the control of the power stroke by strong actin binding.

Keywords: strong binding; actin; myosin cross-bridge; myosin V; decorated actin; cryo-energy-filter electron microscopy

1. THE MYOSIN CROSS-BRIDGE

(a) *Morphology and classification*

The first crystal structure of a myosin cross-bridge (Rayment *et al.* 1993*a*) showed the myosin cross-bridges to be tadpole-like in form (figure 1), with an elongated head, containing a 7-stranded β-sheet and numerous associated α-helices forming a deep cleft at one end of the cross-bridge. The cleft separates two parts of the molecule, which are referred to as the upper 50 K, and lower 50 K domains, both of which are involved in actin binding. The ATP binding site, which lies close to the apex of the cleft, consists of a 'P-loop' motif flanked by switch 1 and switch 2 elements, as are found in the G-proteins. The C-terminal region of the cross-bridge sometimes called the 'neck' but now mostly referred to as the 'lever arm' provides the connection to the thick filament (in myosin II) or to the cargo in non-muscle myosins. This region forms an extended α-helix containing repeated 'IQ motifs' each of which binds a calmodulin-like light chain or calmodulin. In the case of myosin II there are two IQ motifs, in the case of myosin V there are six. The proximal end (as seen from the actin helix) of the extended C-terminal α-helix is anchored in a compact domain (the converter domain) that is attached to the relay helix.

In the meantime approximately 20 structures of the cross-bridge have been solved from various sources and with various ATP analogues bound in the active site. Most structures fall into two classes depending on whether the relay helix has a kink at its middle point or not, and on the position of switch 2. There is a strong correlation between the position of switch 2 and the kink in the relay helix (switch 2 closed—kinked; switch 2 open—straight). We refer to these two classes as pre-power-stroke state and post-rigor state. The post-rigor state was the first structure of the myosin cross-bridge solved and because this crystal structure had no nucleotide in the active site, and it could be fitted into low-resolution electron microscope reconstructions (Rayment *et al.* 1993*b*), it was thought to be a good approximation to the rigor state. However, a structure of the nucleotide-free myosin V cross-bridge has recently been reported that appears to be much closer to the state of myosin in the rigor complex (Coureux *et al.* 2003). This is a new class that breaks the paradigm cited above: the relay helix is straight but the switch 2 element is closed. We will refer to this as rigor-like.

As is discussed by Sweeney & Houdusse (2004), the commonly occurring post-rigor state is likely to be the form of myosin that rapidly releases from actin after the rebinding of ATP at the end of the power stroke (for further discussion see Zeng *et al.* 2004).

* Author for correspondence (holmes@mpimf-heidelberg.mpg.de).

One contribution of 14 to a Discussion Meeting Issue 'Myosin, muscle and motility'.

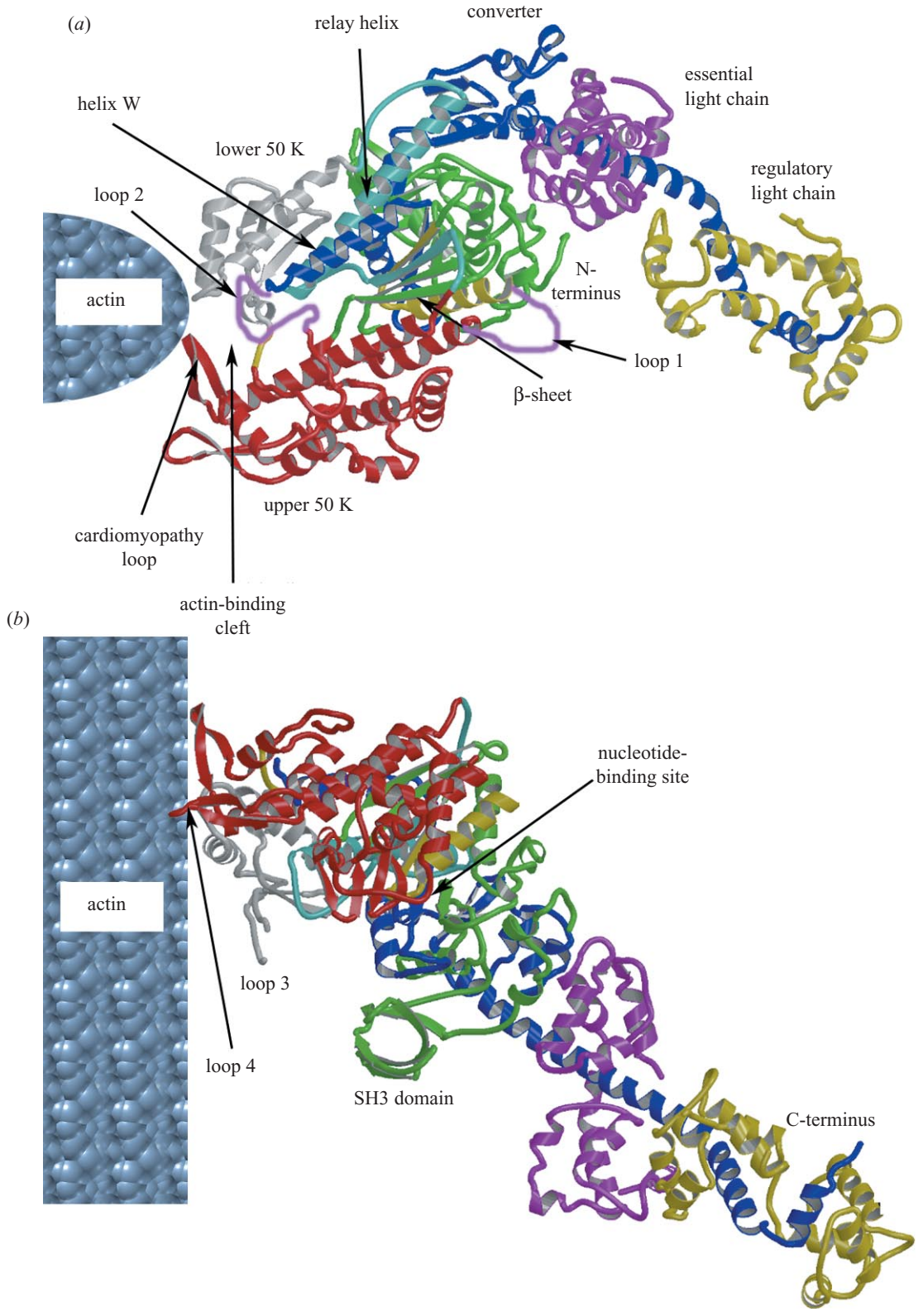

Figure 1. The structure of the myosin cross-bridge (Rayment *et al.* 1993*a*) shown as a ribbon diagram in the orientation it would take on binding to actin viewed (*a*) from the pointed (−)-end of the actin filament and (*b*) at right angles to the actin filament. The N-terminus is coloured green and the nucleotide binding P-loop is coloured yellow; the upper 50 K is coloured red; the lower 50 K domain is coloured grey. Note the cleft separating the upper and lower 50 K domains. The lower 50 K domain appears to be the primary actin-binding site. The upper and lower 50 K domains are also connected by a disordered loop (loop 2—magenta). The C-terminal long helix (dark blue) carries two calmodulin-like light chains and joins onto the thick filament. The relay helix and converter domain are shown. In discussion we refer to proximal or distal as related to the actin helix. This conformation of the cross-bridge (post-rigor state) is close to, but not identical with, the rigor state. The lever arm is in the post-power-stroke position. The colouring is largely historical and does not always correspond with sub-domain boundaries. For example, both helix W and the proximal end of the relay helix are structurally part of the lower 50 K domain.

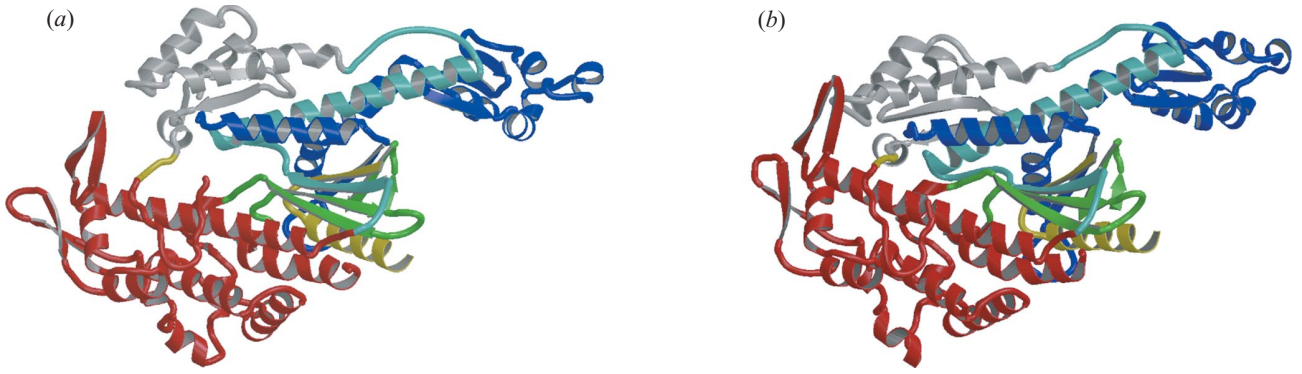

Figure 2. (*a*) Ribbon diagrams of post-rigor myosin II (Rayment *et al.* 1993*a*), and (*b*) rigor-like nucleotide-free myosin V (Coureux *et al.* 2003) in the same orientation as in figure 1*a* (colour coding as in figure 1). Note the closing of the actin-binding cleft. The nucleotide-free myosin V is in the strong actin-binding form.

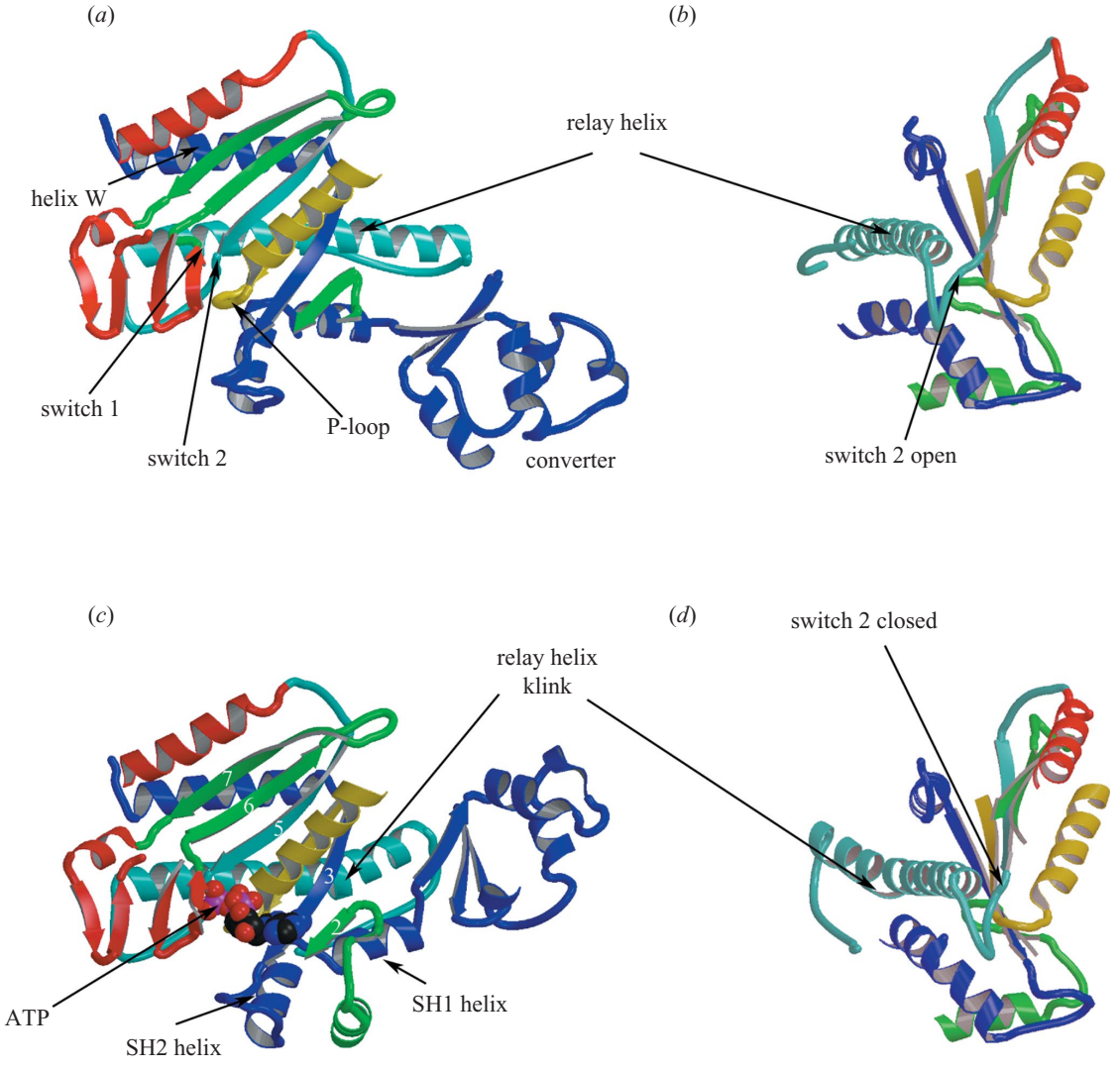

Figure 3. Details of the 7-stranded β-sheet and associated structures (*a*,*b*) in the post-rigor conformation and (*c*,*d*) in the pre-power-stroke conformation. The orientation of (*a*) and (*c*) is close to that shown in figure 1*b*; (*b*) and (*d*) are at right angles to (*a*) and (*c*) looking out from the actin helix. Note the kink in the relay helix in (*c*,*d*) that leads to a 60° rotation of the converter domain. This, in turn, rotates the lever arm 60°. The P-loop (which constitutes the ATP-binding site) and the adjoining α-helix are coloured yellow. The flanking switch sequences (1 and 2) are also shown. The strands of the β-sheet are numbered from the N-terminal (distal) end of the sheet. The lower part of strand 5 (light blue) constitutes switch 2. In the post-rigor state switch 2 lies out of the plane of the β-sheet (open) and in the pre-power-stroke state switch 2 is in the plane of the β-sheet (closed).

2. MYOSIN V

The crystal structure of the cross-bridge of myosin V without bound nucleotide was recently reported (Coureux *et al.* 2003). This construct was truncated just after the first IQ motif defining the first part of the lever arm. The overall atomic structures of myosin II (Rayment *et al.* 1993*a*) and myosin V are similar (figure 2). The most notable difference is in the closing of the actin-binding cleft. Myosin V has a simple one-step, diffusion-limited binding to actin. Thus Coureux *et al.* (2003) have argued that the myosin V nucleotide-free structure is already in the strong binding form, whereas the post-rigor form (e.g. Rayment *et al.* 1993*a*) needs to undergo an isomerization to reach the strong binding geometry. As was first suggested by Rayment *et al.* (1993*b*), it appears that an essential feature of this isomerization is the closing of the actin-binding cleft. These arguments are given in more detail in a companion paper (Sweeney & Houdusse 2004).

(a) *The power stroke and the return of the power stroke*

The essence of the power stroke apparently lies in the formation of the kink in the relay helix at the beginning of the power stroke and the subsequent straightening of the relay helix by removal of the kink. This leads to a 60° rotation of the converter domain and the rotation of the lever arm.

As highlighted by Smith & Rayment (1996) the kink in the relay helix is present in the pre-power-stroke state. By contrast, in the post-rigor state (figure 3) or rigor-like state the relay helix is straight (see review in Geeves & Holmes 1999). The binding of ATP favours the pre-power-stroke state by the interaction of switch 2 with the γ-phosphate. This helps close switch 2. The pre-power-stroke state is also the active form of myosin as an ATPase (Geeves & Holmes 1999; Malnasi-Csizmadia *et al.* 2001). However, the closing of switch 2 and the concomitant moving in (towards the β-sheet) of the lower 50 K domain puts a strain on the relay helix that responds by forming a kink. The kink leads to a rotation of the distal end of the relay helix that in turn rotates the attached converter domain through *ca*. 60° in the plane of the actin filament. This is apparently the return of the power stroke (return stroke).

The presumption has been made that the binding of myosin in the pre-power-stroke conformation to actin reverses this process by allowing the removal of the kink. This would lead to a 60° rotation of the lever arm in the opposite direction (the power stroke). The removal of the strain on the relay helix would apparently be accomplished by moving switch 2 from closed to open. However, the structure of nucleotide-free myosin V (rigor-like) shows that the removal of the strain on the relay helix can also be achieved by bending the β-sheet while leaving switch 2 near to the closed conformation. Therefore, there are now two mechanisms for straightening the relay helix. Closing switch 2 appears to be the pathway for the return stroke. For the power stroke itself, switch 2 is closed in the pre-power-stroke state and is closed in the rigor-like state. Therefore, it seems unlikely that it opens during the power stroke; the power stroke apparently takes place without opening switch 2 appreciably.

(b) *Strong and weak binding to actin*

The second essential property of the myosin cross-bridge is the strong negative coupling between ATP binding and actin binding (for review see Geeves & Conibear 1995). In the absence of ATP the cross-bridge binds with high affinity to the actin filament (rigor-strong binding). The binding of ATP to the myosin cross-bridge leads to a rapid release from actin via formation of the post-rigor structural state (weak binding). Furthermore, the rebinding of the myosin cross-bridge to actin in the pre-power-stroke state, carrying the products of hydrolysis (ADP and phosphate), leads to the release of products; i.e. binding to actin reduces the affinity for nucleotide. One element of the reciprocal coupling of actin affinity and nucleotide affinity appears to be that the switch 1 region moves away from the nucleotide on the closing of the actin binding cleft (Yengo *et al.* 2002; Conibear *et al.* 2003; Holmes *et al.* 2003); and the binding of ATP opens the cleft and reduces the affinity for actin vice versa.

3. ACTIN COORDINATES

Actin has two conformations, g (globular) and f (fibrous). Crystal structures are available for only the g-form. The only high-resolution data available for f-actin are from fibre diffraction patterns (Holmes *et al.* 1990). Several attempts have been made to fit a helix of g-actin monomers to the observed f-actin fibre diffraction pattern by refinement methods (Holmes *et al.* 1990; Lorenz *et al.* 1993; Tirion *et al.* 1995). Because the fibre diffraction patterns are of limited resolution (6–8 Å) the refinement is underdetermined. As a result, these various methods produce related but different answers. In the present study, the four sub-domains of g-actin (Kabsch *et al.* 1990) were allowed to move as independent solid bodies to minimize the difference between the calculated fibre diffraction pattern and the observed fibre diffraction pattern. The starting structure was the structure of g-actin from Otterbein *et al.* (2001) but with the sub-domains positioned approximately over the corresponding parts of the Lorenz structure (Lorenz *et al.* 1993). The loop containing the methyl-histidine (72–80) was also allowed to refine separately. The sub-domains were constrained to remain connected. After the refinement, the stereochemistry of residues in the junction regions was repaired by use of the program CNS (Brunger *et al.* 1998). The method is rather sensitive to the starting coordinates. The final quadratic *R*-value was 8% out to a resolution of 8 Å. The refined structure has much in common with the Lorenz structure except at the interface between sub-domain 2 and sub-domain 1 in the neighbouring molecule. The 40–50 α-helix in sub-domain 2 of the Otterbein structure builds a better interface than could be obtained from the previous structures of g-actin.

Because the oriented gels were obtained from phalloidin-labelled actin, phalloidin was included in the refinement. The coordinates of the phalloidin molecule were taken from a crystal structure determination of a phalloidin analogue (Falcigno *et al.* 2001). The coordinates of the missing side chain of the dihydroxyleucine were supplied by model building. Owing to the limited resolution of the fibre diffraction pattern only the *x*, *y*, *z* coordinates of the centre of gravity of the phalloidin were refined. The orientation of the phalloidin is arbitrary.

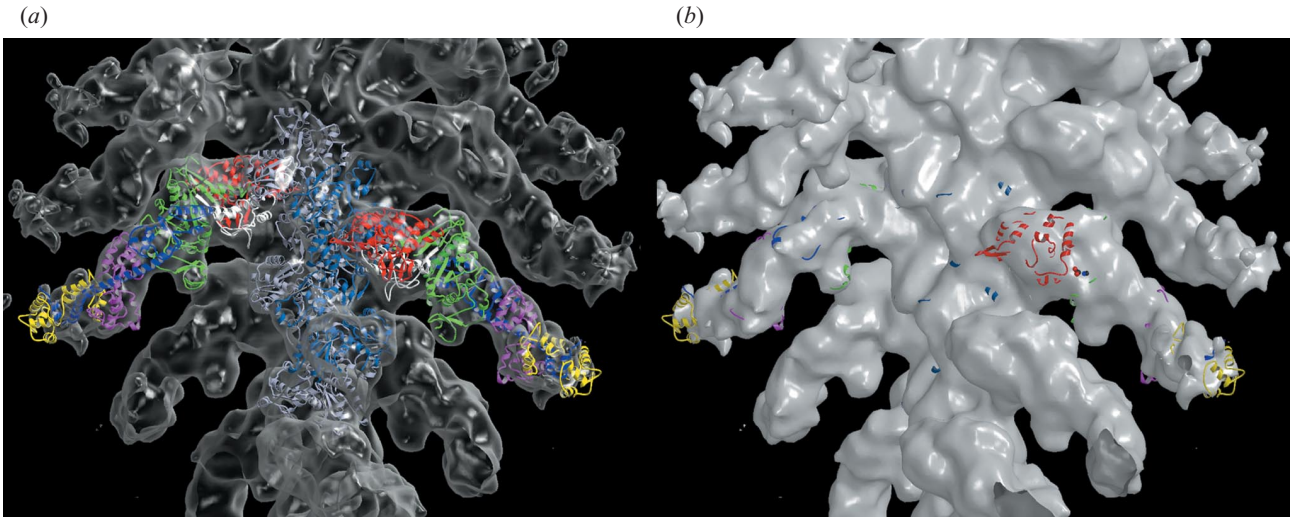

Figure 4. Fit of crystallographic molecular models of f-actin and myosin subfragment-1 into the reconstructed density. The molecular models of myosin and f-actin are shown docked into the experimental density (electron cryo-microscopy reconstruction). Fitting was achieved by use of an iterative least-squares algorithm. (*a*) General fit of f-actin and myosin (two cross-bridges are shown). Here, myosin has been kept in its original X-ray crystallographic conformation (post-rigor). The density contoured at 2σ is shown as transparent. (*b*) The same but with a solid surface. The surface representation illustrates the localized poor fit of the myosin upper 50 kDa domain (shown in red) that protrudes out of the density.

4. CRYO-ENERGY-FILTERED ELECTRON MICROSCOPY OF DECORATED ACTIN

Studies of the actin–myosin cross-bridge complex by cryo-energy-filtered electron microscopy (Holmes *et al.* 2003) have yielded higher-resolution structural data on the actin–myosin interaction. Zero-loss energy-filtered imaging dramatically improves the signal : noise ratio in the micrographs and, moreover, allows an accurate correction for the CTF. The improved signal : noise ratio also allows better alignment procedures during image processing, which yield improved resolution and therefore allow a more detailed description of the actin–myosin interaction. The improvement in signal : noise ratio arising from using the energy-filter allowed data to be taken rather close to focus and at a relatively low electron dose. Moreover, an algebraic method of 3D reconstruction (filtered least-squares) allows one to determine the density at chosen points. Because of the asymmetric shape of decorated actin this procedure halves the number of lattice points at which the density has to be determined, which leads to a concomitant increase in precision. By merging focal series at four different degrees of under focus and after correcting for the CTF, the density shown in figure 4 was obtained. The resolution of the map was 14 Å. Shown fitted into the map in figure 4 are the atomic models of f-actin and the crystal structure of the chicken skeletal myosin II cross-bridge from Rayment *et al.* (1993*a*) (post-rigor state). Figure 4*a* shows the satisfactory overall fit obtained with the Rayment model showing that this model is close to the rigor state of the myosin cross-bridge. However, in figure 4*b* it can be seen that to fit the map some modifications are necessary: the upper 50 K domain (red) is not contained within the 2α contour level of the map. Holmes *et al.* (2003) showed that by allowing the upper 50 K domain to move freely the Rayment post-rigor structure could be modified to fit within the 2α contour of the electron micrograph reconstruction. The actin-binding cleft was shown to close on strong binding to actin with a concomitant movement of the switch 1 region that opened the nucleotide-binding pocket.

5. FITTING MYOSIN V INTO THE MAP

We calculated a *rigid body* fit of the truncated myosin V motor domain into the electron microscope density of myosin II decorated actin. The missing structures (the lever and part of the N-terminus) were provided from myosin II coordinates and allowed to refine independently. Their presence or absence had no significant effect on the position of truncated myosin V. A very good fit was obtained, most of the molecules lie within the 2.5α contour (figure 5). This is a much better result than can be obtained by a simple rigid body fit of post-rigor myosin II into the density. Nor does the fit generate difference densities peaks (such peaks were a prominent feature of attempts to fit the post-rigor structure), which indicates that no prominent shifts of parts of the molecule are required to produce a fit.

6. THE ACTIN–MYOSIN INTERFACE

The fit of the myosin V crystal structure into the electron microscopy map produces no steric clashes and several hydrophobic residues on both sides of the interface come into proximity. Figure 6 shows a ribbon diagram of the actin–myosin interface. In figure 6, the myosin residues involved in the interface are coloured yellow. The actin residues in the interface are cyan.

The actin–myosin interface has two distinct parts. The more substantial interface is provided by the lower 50 K domain: the interaction of the helix-turn-helix 499–532 (526–559 chicken) in the lower 50 K domain with the actin residues helix 337–351 and the short helix-turn 140–149. The actin residues involved in the interaction are leu140, tyr143, ile341, ile345, leu349, phe352 and possibly phe375. The myosin residues involved for myosin V are: lys502, met503, glu511, lys514, met515, pro516; and chicken skeletal myosin II are: pro529, met530, glu538, met541, phe542, pro543.

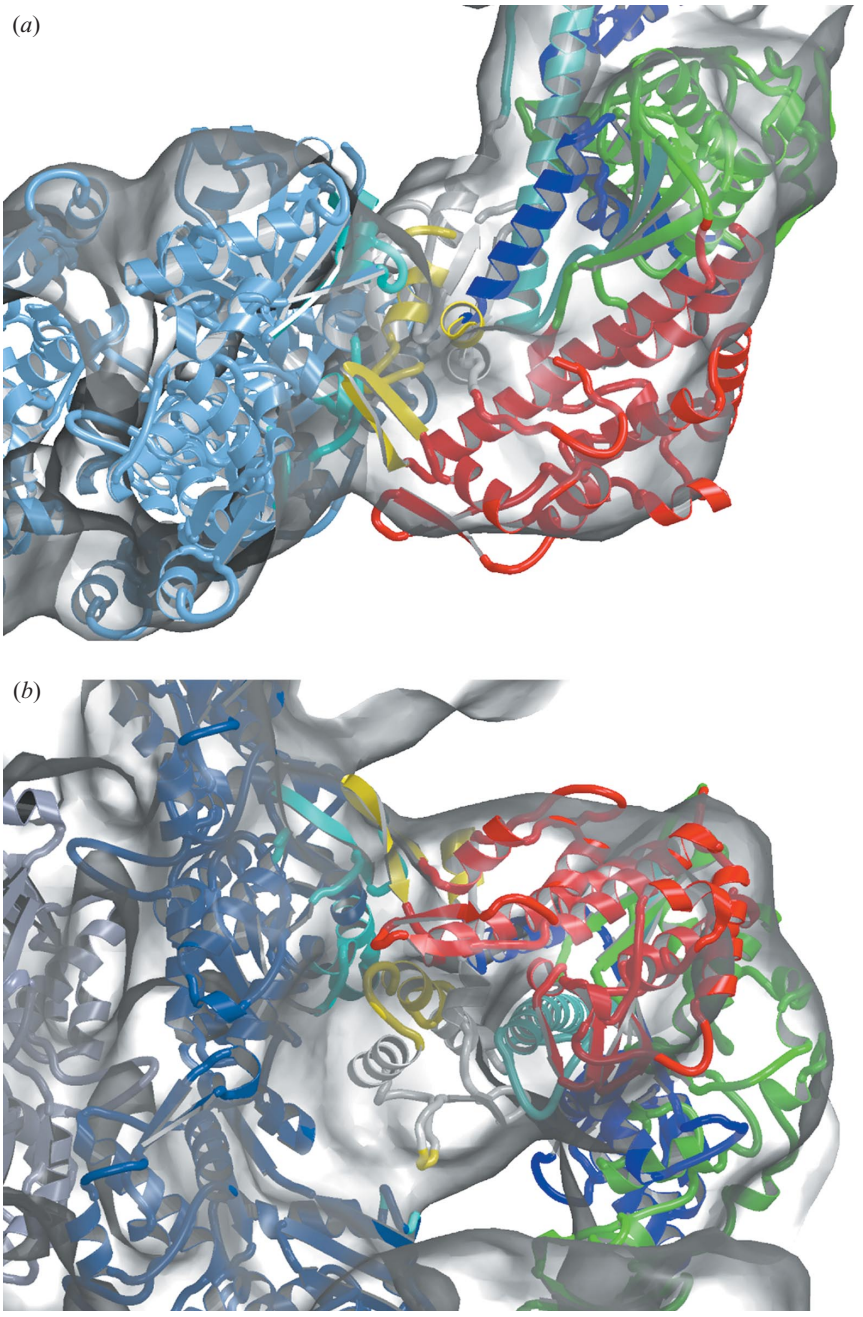

Figure 5. (*a*) View looking down the actin helix with the electron microscope 3D reconstruction density contoured at 2.5σ. The actin is to the left. The myosin is colour coded as in figure 1. The myosin residues involved in the interface are coloured yellow. The actin residues in the interface are coloured cyan. (*b*) View at right angles to the actin helix.

The second part of the binding site is made by the cardiomyopathy loop. The actin residues involved in the interaction are between pro333 to tyr337 and ala26 to ala29. The cardiomyopathy loop of myosin V lies in a good orientation to make this interaction without a major rearrangement whereas the cardiomyopathy loop of myosin II would have to untwist. The residues involved lie between 380 and 389 in myosin V. It is also possible that the so-called loop 4 (residues 342–349 in myosin V) reorganizes to become part of this binding site. Both parts of the main binding site lie on the same actin monomer although it appears likely that loop 3 (540–544) in myosin V (and other myosins) makes a weak secondary contact with the neighbouring actin monomer near the actin residues 95–100. (Note that the corresponding loop in chicken myosin is disordered in the crystal structure.) Note also that the N-terminal end of loop 2 that contains basic residues is found close to acidic residues of the sub-domain 1 of actin (residues 1–4, 24–25). Although loop 2 makes important contributions to actin interactions that affect both of the product release steps (Joel *et al.* 2001, 2003; Yengo & Sweeney 2004), it is not clear how specific or critical any of these interactions are to the rigor interface. The first two to three residues that start loop 2 may be in electron microscope density but most of loop 2 is not visible and seems to be disordered.

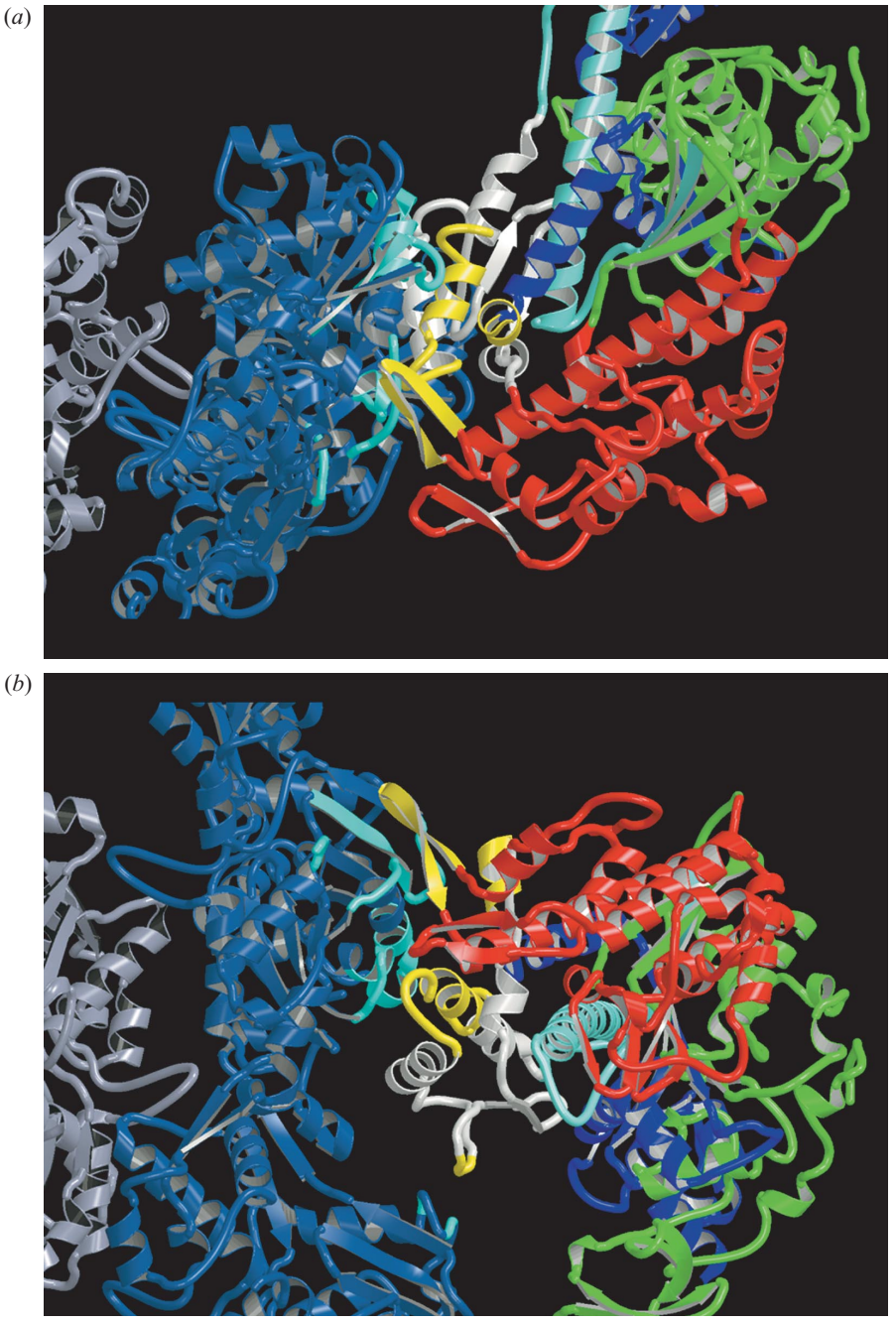

Figure 6. Myosin V docked onto actin. Actin is to the left. (*a*) View along the actin filament. (*b*) View at right angles to the actin filament. Colour coding as in figure 1. The myosin residues involved in the interface are coloured yellow. The actin residues in the interface are coloured cyan. There are two major sites, the lower 50 K domain and the cardiomyopathy loop that interact with the same actin monomer. There is also a minor site made by loop 3 that contacts the next actin down. The residues are listed in § 6.

7. DISCUSSION

(a) *Models of pre- and post-power stroke for myosin II*

By overlaying the converter domains one can augment the truncated myosin V with the lever arm from chicken skeletal myosin II (Protein Data Bank 2MYS). The resulting lever arm fits the electron micrograph reconstruction very well although these data were not used in fitting the truncated myosin V into the density map. Therefore, by combining myosin V with myosin II we seem to be able to generate a good model of post-power-stroke myosin II. This is shown in figure 7*b*.

Model building of the pre-power stroke is not so clear. There are three well-defined pre-power-stroke structures in the literature (scallop adductor myosin; Houdusse *et al.* 2000), truncated chicken smooth muscle myosin II (two forms; Dominguez *et al.* 1998) and truncated *Dictyostelium* myosin II (Smith & Rayment 1996). (We have used the very similar m754 that has a better defined converter domain; F. Jon Kull, private communication.) The primary binding site between the myosin cross-bridge and actin appears to be the lower 50 K domain. To obtain an estimate of the pre-power-stroke state when attached to actin we may assume that the geometry of the lower 50 K domain binding to actin is fairly constant and superimpose

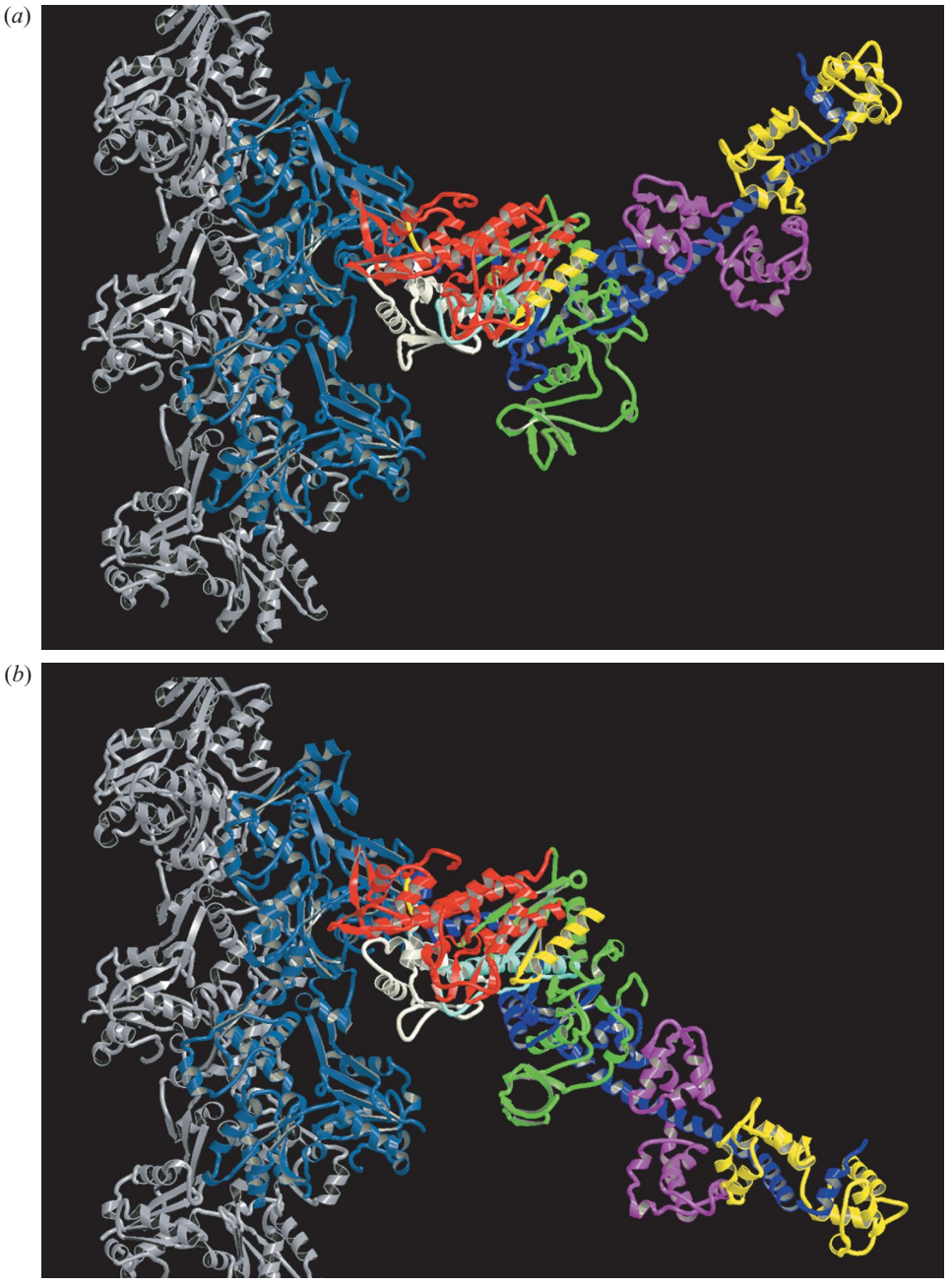

Figure 7. Models of the (*a*) pre- and (*b*) post-power-stroke states of myosin II (for details see § 7a).

each of the pre-power-stroke myosins on the lower 50 K domain of the attached myosin V. All three superpositions give virtually the same answer. Differences begin at the distal end of the relay helix. The converter domain orientations are separated by *ca*. 3°. In all three the C-terminal helix sets off in approximately the same direction (within 3°) but then in smooth muscle the helix breaks to head off vertically whereas the scallop lever arm, by virtue of its interactions with the second light chain, bends round so as to point horizontally. Which set of data would be relevant for the myosin II pre-power stroke?

Before the break in the smooth muscle C-terminal helix, the smooth and *Dictyostelium* models are rather alike. However, the break in the smooth muscle helix was not indicated in solution studies on smooth muscle S1, in which the lever arm position in actin- and non-actin-bound was sensed with energy transfer (LRET, lanthanide resonance energy transfer). In that case, the distance between the regulatory light chain and the motor domain was consistent with a straight C-terminal helix (Xiao *et al.* 2003). It is possible that this break results from crystal-packing forces in the crystal structure (Dominguez *et al.* 1998) or it may indicate a flexibility that is useful for allowing cross-bridges to bind to actin more easily in the pre-power-stroke conformation. By contrast, the scallop-specific bent lever arm is not appropriate (the bent lever arm would not fit the rigor electron microscope data), and is likely to be a peculiarity owing to the calcium regulatory site in that myosin (which has essential light chain and regulatory light chain contributions; Houdusse *et al.* 2000). Therefore the most appropriate model for the chicken skeletal muscle cross-bridge pre-power-stroke state is to take the straight

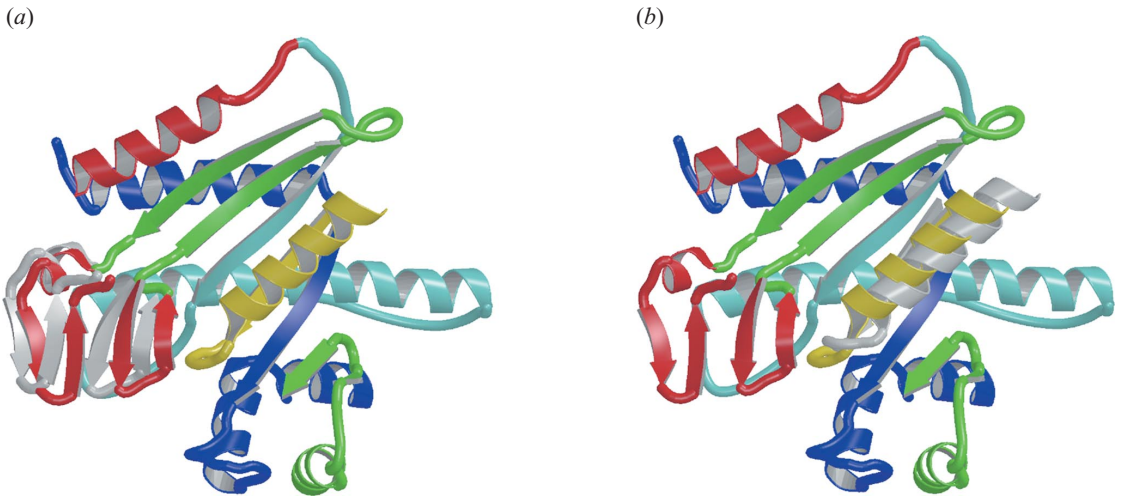

Figure 8. (*a*) The movement of switch 1 between the post-rigor state (red) and myosin V (grey), which is taken as the rigor state. (*b*) The movement of the P-loop post-rigor (yellow) and rigor-like myosin V (grey). The orientation is the same as in figure 2*a*.

C-terminal helix and build on the skeletal muscle myosin II lever arm. The result is shown in figure 7*a*. From this model, one sees that in myosin II the lever arm swings from *ca*. $+30^{\circ}$ to -30°.

(b) *Movement of switch 1*

The closing of the actin-binding cleft on strong binding to actin opens switch 1, which opens the nucleotide-binding site. This movement appears to be an important part of the strong inverse linkage between the binding of actin to the myosin cross-bridge and the binding of nucleotide. An estimate of the magnitude of this movement can be obtained by comparing the rigor-like myosin V structure with post-rigor myosin II. To make this comparison, we have overlaid residues at the proximal end of the central β-sheet because this overlay appears to conserve the local geometry of the nucleotide-binding pocket. Switch 1 is embedded in a small sub-domain consisting of a four-stranded β-sheet. The movement of this β-sheet between myosin II and myosin V is shown in figure 8*a*. The movement of switch 1 at Arg239 is 3.2 Å and for Asn242 1.8 Å (chicken sequence). Although these movements are about half those estimated from electron microscopy (Holmes *et al.* 2003), they are still substantial enough to enable hydration of the nucleotide and thereby facilitate its release.

The second and remarkable effect is that whole of the P-loop moves upwards *ca*. 5.0 Å to destroy the nucleotide-binding pocket (Sweeney & Houdusse 2004). This is depicted in figure 8*b*. The movement is linked to a twist in the distal part of the β-sheet. In a recent crystal structure of a nucleotide-free truncated *Dictyostelium* myosin II, Reubold *et al.* (2003) report a similar movement of the P-loop.

(c) *Implications for the power stroke*

One remarkable feature of the myosin V structure is that the switch 2 element and the associated lower 50 K domain are in conformations similar to the so-called 'closed conformation', which until now has been associated with the pre-power-stroke state of the myosin head (Geeves & Holmes 1999). Since the switch 2 element is closed in the pre-power-stroke state and is now seen to be essentially closed in the rigor-like state, the implication is that it is closed for the whole of the power stroke.

The closing of switch 2 was thought to be necessary and sufficient for the 'kinking' of the relay helix that produces the pre-power-stroke conformation of the converter domain. Despite switch 2 being closed, in the myosin V structure the relay helix is 'straight' and the converter domain is in the post-power-stroke position. However, an important new property of myosin is the twisting of the central β-sheet, which until the nucleotide-free myosin V structure (Coureux *et al.* 2003) and the nucleotide-free truncated *Dictyostelium* myosin II (Reubold *et al.* 2003) had not been seen. The twist explains how it is possible to reach the post-power stroke ('straight' relay helix) while the lower 50 K domain remains close to the 'closed' configuration: the twisting of the β-sheet relieves pressure on the kinked relay helix by rotating strand 3 of the sheet and the attached SH1 and SH2 helices. This allows the relay helix to straighten and to reach the post-power-stroke conformation while retaining a closed geometry for switch 2. The origin of the twisting of the β-sheet is discussed in the accompanying paper (Esnouf 1997, 1999; Sweeney & Houdusse 2004).

The fact that the twisting of the β-sheet *can* lead to a straightening of the relay helix suggests a mechanism whereby actin binding might control the power stroke. If closure of the actin-binding cleft leads to a mandatory twisting of the β-sheet then the binding of actin would be the cause of the power stroke. This alone does not explain the transition weak-to-strong nor does it explain the ordered release of products. The opening of the nucleotide-binding site appears to be associated with movements of switch 1 and the P-loop.

8. PREPARATION OF FIGURES

The following programs have been used in preparing the figures: BobScript v2.6 (Esnouf 1997, 1999), Molscript (Kraulis 1991), Raster 3D (Merritt & Bacon 1997).

The authors thank Susanne Eschenburg for her help in refining the actin structure.

REFERENCES

Brunger, A. T. (and 13 others) 1998 Crystallography & NMR system: a new software suite for macromolecular structure determination. *Acta Crystallogr. D* **54**, 905–921.

Conibear, P. B., Bagshaw, C. R., Fajer, P. G., Kovacs, M. & Malnasi-Csizmadia, A. 2003 Myosin cleft movement and its coupling to actomyosin dissociation. *Nature Struct. Biol.* **10**, 831–835.

Coureux, P. D., Wells, A. L., Menetrey, J., Yengo, C. M., Morris, C. A., Sweeney, H. L. & Houdusse, A. 2003 A structural state of the myosin V motor without bound nucleotide. *Nature* **425**, 419–423.

Dominguez, R., Freyzon, Y., Trybus, K. M. & Cohen, C. 1998 Crystal structure of a vertebrate smooth muscle myosin motor domain and its complex with the essential light chain: visualization of the pre-power stroke state. *Cell* **94**, 559–571.

Esnouf, R. M. 1997 An extensively modified version of MolScript that includes greatly enhanced coloring capabilities. *J. Mol. Graph Model.* **15**, 112–113.

Esnouf, R. M. 1999 Further additions to MolScript version 1.4, including reading and contouring of electron-density maps. *Acta Crystallogr. D* **55**, 938–940.

Falcigno, L., Costantini, S., D'Auria, G., Bruno, B. M., Zobeley, S., Zanotti, G., Paolillo, L., Saviano, M. & Campanile, T. 2001 Phalloidin synthetic analogues: structural requirements in the interaction with F-actin. Solid state and solution conformation of [Ala(7)]-phalloidin: a synthetic phallotoxin analogue. *Chem. A Eur. J.* **7**, 4665–4673.

Geeves, M. A. & Conibear, P. B. 1995 The role of three-state docking of myosin S1 with actin in force generation. *Biophys. J.* **68**, 194S–201S.

Geeves, M. A. & Holmes, K. C. 1999 Structural mechanism of muscle contraction. *A. Rev. Biochem.* **68**, 687–727.

Holmes, K. C., Popp, D., Gebhard, W. & Kabsch, W. 1990 Atomic model of the actin filament. *Nature* **347**, 44–49.

Holmes, K. C., Angert, I., Kull, F. J., Jahn, W. & Schroder, R. R. 2003 Electron cryo-microscopy shows how strong binding of myosin to actin releases nucleotide. *Nature* **425**, 423–427.

Houdusse, A., Szent-Gyorgyi, A. G. & Cohen, C. 2000 Three conformational states of scallop myosin S1. *Proc. Natl Acad. Sci. USA* **97**, 11 238–11 243.

Joel, P. B., Trybus, K. M. & Sweeney, H. L. 2001 Two conserved lysines at the 50/20-kDa junction of myosin are necessary for triggering actin activation. *J. Biol. Chem.* **276**, 2998–3003.

Joel, P. B., Sweeney, H. L. & Trybu, K. M. 2003 Addition of lysines to the 50/20 kDa junction of myosin strengthens weak binding to actin without affecting the maximum ATPase activity. *Biochemistry* **42**, 9160–9166.

Kabsch, W., Mannherz, H. G., Suck, D., Pai, E. F. & Holmes, K. C. 1990 Atomic structure of the actin:DNase I complex. *Nature* **347**, 37–44.

Kraulis, P. J. 1991 MolScript: a program to produce both detailed and schematic plots of proteins structures. *J. Appl. Crystallogr.* **24**, 946–950.

Lorenz, M., Popp, D. & Holmes, K. C. 1993 Refinement of the F-actin model against X-ray fiber diffraction data by the use of a directed mutation algorithm. *J. Mol. Biol.* **234**, 826–836.

Malnasi-Csizmadia, A., Pearson, D. S., Kovacs, M., Woolley, R. J., Geeves, M. A. & Bagshaw, C. R. 2001 Kinetic resolution of a conformational transition and the ATP hydrolysis step using relaxation methods with a *Dictyostelium* myosin II mutant containing a single tryptophan residue. *Biochemistry* **40**, 12 727–12 737.

Merritt, E. A. & Bacon, D. J. 1997 Raster3D version 2: photorealistic molecular graphics. *Meth. Enzymol.* **277**, 505–524.

Otterbein, L. R., Graceffa, P. & Dominguez, R. 2001 The crystal structure of uncomplexed actin in the ADP state. *Science* **293**, 708–711.

Rayment, I., Rypniewski, W. R., Schmidt-Base, K., Smith, R., Tomchick, D. R., Benning, M. M., Winkelmann, D. A., Wesenberg, G. & Holden, H. M. 1993*a* Three-dimensional structure of myosin subfragment-1: a molecular motor. *Science* **261**, 50–58.

Rayment, I., Holden, H. M., Whittaker, M., Yohn, C. B., Lorenz, M., Holmes, K. C. & Milligan, R. A. 1993*b* Structure of the actin–myosin complex and its implications for muscle contraction. *Science* **261**, 58–65.

Reubold, T. F., Eschenburg, S., Becker, A., Kull, F. J. & Manstein, D. J. 2003 A structural model for actin-induced nucleotide release in myosin. *Nature Struct. Biol.* **10**, 826–830.

Smith, C. A. & Rayment, I. 1996 X-ray structure of the magnesium(ii).adp.vanadate complex of the dictyostelium-discoideum myosin motor domain to 1.9 Å resolution. *Biochemistry* **35**, 5404–5417.

Sweeney, H. L. & Houdusse, A. 2004 The motor mechanism of myosin V: insights for muscle contraction. *Phil. Trans. R. Soc. B* **359**, 1829–1842. (doi:10.1098/rstb.2004.1576)

Tirion, M. M., ben-Avraham, D., Lorenz, M. & Holmes, K. C. 1995 Normal modes as refinement parameters for the F-actin model. *Biophys. J.* **68**, 5–12.

Xiao, M., Reifenberger, J. G., Wells, A. L., Baldacchino, C., Chen, L. Q., Ge, P., Sweeney, H. L. & Selvin, P. R. 2003 An actin-dependent conformational change in myosin. *Nature Struct. Biol.* **10**, 402–408.

Yengo, C. M. & Sweeney, H. L. 2004 Functional role of loop 2 in myosin V. *Biochemistry* **43**, 2605–2612.

Yengo, C. M., De la Cruz, E. M., Chrin, L. R., Gaffney, D. P. & Berger, C. L. 2002 Actin-induced closure of the actin-binding cleft of smooth muscle myosin. *J. Biol. Chem.* **277**, 24114–24119.

Zeng, W., Conibear, P. B., Dickens, J. L., Cowie, R. A., Wakelin, S., Málnási-Csizmadia, A. & Bagshaw, C. R. 2004 Dynamics of actomyosin interactions in relation to the crossbridge cycle. *Phil. Trans. R. Soc. B* **359**, 1843–1855. (doi:10.1098/rstb.2004.1527)

GLOSSARY

CTF: contrast transfer function